



City Research Online

City, University of London Institutional Repository

Citation: Gruppetta, S., Koechlin, L., Lacombe, F. & Puget, P. (2005). Curvature sensor for the measurement of the static corneal topography and the dynamic tear film topography in the human eye. *Optics Letters*, 30(20), pp. 2757-2759. doi: 10.1364/ol.30.002757

This is the unspecified version of the paper.

This version of the publication may differ from the final published version.

Permanent repository link: <https://openaccess.city.ac.uk/id/eprint/1512/>

Link to published version: <https://doi.org/10.1364/ol.30.002757>

Copyright: City Research Online aims to make research outputs of City, University of London available to a wider audience. Copyright and Moral Rights remain with the author(s) and/or copyright holders. URLs from City Research Online may be freely distributed and linked to.

Reuse: Copies of full items can be used for personal research or study, educational, or not-for-profit purposes without prior permission or charge. Provided that the authors, title and full bibliographic details are credited, a hyperlink and/or URL is given for the original metadata page and the content is not changed in any way.

City Research Online:

<http://openaccess.city.ac.uk/>

publications@city.ac.uk

A curvature sensor for the measurement of the static corneal topography and the dynamic tear film topography in the human eye

Steve Gruppetta

*Laboratoire d'Etudes Spatiales et d'Instrumentation en Astrophysique, Observatoire de Paris,
5, place Jules Janssen, 92195 Meudon, France*

Laurent Koechlin

*Laboratoire d'Astrophysique de Toulouse, Observatoire Midi Pyrénées,
14, avenue Edouard Belin, 31400 Toulouse, France*

François Lacombe and Pascal Puget

*Laboratoire d'Etudes Spatiales et d'Instrumentation en Astrophysique, Observatoire de Paris,
5, place Jules Janssen, 92195 Meudon, France*

A system to measure non-invasively the topography of the first optical surface of the human eye using a curvature sensor is described. The static corneal topography and the dynamic topography of the tear film can both be measured and the topographies obtained are presented. The system makes possible the study of the dynamic aberrations introduced by the tear film to determine their contribution to the overall ocular aberrations in healthy eyes, eyes with corneal pathologies and eyes wearing contact lenses. © 2005 Optical Society of America

OCIS codes: 170.0170, 330.0330, 010.1080, 170.3890, 170.4460, 170.4470, 330.5370.

The optical surface of the cornea contributes considerably to the aberrations introduced by the optics of the human eye. The interest in the dynamic component of the ocular aberrations has increased mostly due to the rapid advancement of adaptive optics for retinal imaging and psychophysics, where the ocular aberrations are measured and corrected with adaptive devices in real time in order to achieve higher resolution. Suggestions have been made that

the tear film on the corneal surface, being a liquid layer, could significantly affect these changing aberrations.¹ A better knowledge of the dynamics of tear film aberrations, and of ocular aberrations as a whole, is essential for the next generation of adaptive optics systems. The dynamic tear film topography has only recently started being studied.² It is also of particular interest in the study of contact lens fitting because of the perturbation caused to the tear film layer.

A curvature sensor is presented in this Letter with which the topography of the first optical surface in the eye can be measured both statically and dynamically. Such a system offers increased lateral and height resolution with respect to standard corneal topographers, notably placido disk systems, since it is in principal limited by the size of cornea represented by 1 CCD pixel ($(50 \times 50)\mu\text{m}$) and the bit resolution of the cameras. Curvature sensing also offers more reliable wavefront reconstruction than that reported for other interferometric systems². The local curvature of the wavefront at the pupil plane (the plane which includes the interface between air and the tear film) can be obtained by measuring the changes in local intensity which arise due to propagation of the beam.^{3,4} Thus, if the intensity at the pupil (at $z = 0$) having a transmission function $P(x, y)$ is I_0 , then the intensities at two planes which are at an axial distance of $+\Delta z$ and $-\Delta z$ respectively from the pupil plane are given by

$$I_1 = I_0 + \frac{\partial I}{\partial z} \Delta z, \quad (1)$$

$$I_2 = I_0 - \frac{\partial I}{\partial z} \Delta z, \quad (2)$$

for a paraxial beam propagating in the z -direction. We can use the irradiance transport equation for phase retrieval,⁵ so that

$$\frac{\partial I}{\partial z} = -\nabla I \cdot \nabla W - I \nabla^2 W, \quad (3)$$

where the intensity $I \equiv I(x, y, z)$, the wavefront $W \equiv W(x, y, z)$ and the operator $\nabla \equiv (\partial/\partial x, \partial/\partial y)$. Assuming uniform illumination within the pupil and no illumination elsewhere, then ∇I is non-zero only at the pupil edge, and if \mathbf{n} is the outward unit vector perpendicular to the pupil edge and δ_c is the Dirac delta function defined on the same pupil edge, then $\nabla I = -I_0 \mathbf{n} \delta_c$.

The signal S of the curvature sensor is the normalised difference of the two intensity measurements:

$$S = \frac{I_1 - I_2}{I_1 + I_2} = \left(\frac{\partial W}{\partial n} \delta_c - P \nabla^2 W \right) \Delta z. \quad (4)$$

The wavefront is retrieved by solving the above Poisson equation using the Neumann boundary conditions. As a first approximation, the signal is taken to be the Laplacian of the wavefront and the first estimate of the wavefront is obtained by solving in the Fourier domain.

Since the Laplacian operator ∇^2 is equivalent to a multiplication by $(u^2 + v^2)$ in the Fourier domain, where u and v are the coordinates in the Fourier domain, then the Fourier transform of the sensor signal is divided by $(u^2 + v^2)$ and the inverse Fourier transform is calculated. An adjustable Hanning window is applied to reduce high frequency noise. Since the sensor signal, however, is the Laplacian multiplied by the pupil function, the wavefront W obtained is only an approximation and the signal boundaries should be taken into account. This is done by using a Gershberg-type algorithm.⁶ The algorithm sets constraints to the wavefront at each iteration, both in the direct space and in the Fourier space. In the direct space, $\partial W/\partial x$ and $\partial W/\partial y$ are computed from the approximate wavefront W in a narrow band outside the signal boundaries and then $\partial W/\partial n$ is set equal to zero so that only the tangential component of the gradient remains in this band. This satisfies the Neumann boundary condition required. The Laplacian of this band outside the boundaries is then calculated. The original signal is placed within the signal boundaries and this modified sensor signal with extrapolated boundaries is used to iterate the procedure. Thus, in the Fourier domain, the modulus is constrained to the values obtained from the actual measurements, except at very low frequencies. Iterations are repeated until the wavefront converges to within the desired error.

The optical system used is shown in Fig. 1. A halogen lamp is used as an incoherent light source with a filter which transmits lights at $(600 \pm 40)\text{nm}$. The light intensity incident on the cornea is 400nW , well below the safety levels established by the European standard EN 60825-1;1994. A collector lens focuses the light onto a pinhole and a 70:30 beamsplitter couples the light onto a photographic objective lens ($f = 50\text{mm}$, $f/1.2$) which focuses the light onto the centre of curvature of the subject's cornea. The light reflected from the interface between the air and the tear film follows a return path identical to the incident beam, though the wavefront is aberrated due to the deviation of the tear film surface from a perfect sphere. This reflected beam is split by a 50:50 beamsplitter and two achromatic doublets ($f = 50\text{mm}$) are used to collimate the beams onto two CCD cameras. The distances between the collimating lenses and the CCD cameras are set such that the cameras are conjugate to planes which are at $+\Delta z$ and $-\Delta z$ respectively from the plane containing the air-tear film interface. Δz is proportional to the contrast ϵ between the intensity at the two measuring planes, and inversely proportional to the local curvature C , and is given by $\Delta z = \epsilon/2C$.³ The smallest detectable curvature value was chosen to be $C = 8\text{m}^{-1}$ which corresponds to an elevation of $0.01\mu\text{m}$ over a corneal area of $(50 \times 50)\mu\text{m}$ corresponding to one CCD pixel. Using a contrast of $\epsilon = 5\%$ which is determined by the noise level of the CCD cameras, we obtain a value for Δz of 3mm . Larger curvatures will produce a higher contrast for this value of Δz and will thus be detected. Since equations 1 and 2 are exact only in the limit $\Delta z \rightarrow 0$, accuracy in the wavefront reconstruction is lost as Δz increases, hence the smallest value obtained above will be used.

A one-off calibration was achieved first by placing a plane mirror at the focus of the objective to measure aberrations inherent to the optical system, then by measuring surfaces of known topographies. The measurement error of the setup is of $0.005\mu\text{m}$, an accuracy of $0.08\mu\text{m}$ and a repeatability between measurements of $0.02\mu\text{m}$. The system was used to measure either the static corneal topography or the dynamic topography of the tear film on human eyes. Using a chin rest and head support (supporting the forehead and the sides of the head), the subjects were aligned and instructed to fixate a target shown on a computer screen. For the static topography measurement, series of 30 sets of intensity measurements were taken (the acquisition time being less than 2s) and averaged. For the dynamic topography, series were recorded over a typical interval of 10s at a frequency of 20Hz. The sensitivity of the system to lateral eye movements facilitated the removal of frames from the series which correspond to moments during the acquisition period in which the eye was off axis. The illuminated pupil on the cornea had a 4mm diameter.

Fig. 2 shows the corneal topography of an astigmatic eye obtained from the system. The topography map is represented in terms of the radial curvature, this being the preferred representation for corneal topography in ophthalmology. Fig. 3 shows individual frames from series of tear film topographies. For displaying tear film maps, the representation of the wavefront map itself was chosen after first and second order Zernike terms had been removed. Fig. 3(a) represents a frame which just precedes a blink, showing wrinkle-like features produced as the top and bottom eye lids were pushing on the tear film as they were closing. Fig. 3(b) shows the presence of a small bubble in the tear film, $0.2\mu\text{m}$ in height, probably due to a foreign particle on the cornea.

The effect of the tear film on the transmitted wavefront through the optics of the eye can be represented by monitoring the evolution of the RMS error of the wavefront over time, as shown in Fig. 4. During the 10s-series shown in Fig. 4(a), the subject blinked three times. It can be noticed that there is an increase in the RMS wavefront error preceding a blink caused by the disruption to the tear film as shown in Fig. 3(a). On the other hand, Fig. 4(b) represents another 10s-series in which the subject refrained from blinking. We are currently collecting extensive series of data with the system described in this Letter from a group of healthy eyes, which include contact lens wearers, in order to determine whether the tear film contributes significantly to the dynamic ocular aberrations. These results will be published separately.

We have applied curvature sensing to measure the topography of the cornea and the tear film non-invasively using a simple optical arrangement. The system is being used for further studies of the tear film aberrations.

Steve Gruppeta is funded by the European Union Research and Training Network

SHARP-EYE, contract number HPRN-CT-2002-00301. Steve Gruppetta's email address is steve.gruppetta@obspm.fr.

References

1. H. Hofer, P. Artal, B. Singer, J. L. Aragón, and D. R. Williams, "Dynamics of the eye's wave aberration," *J. Opt. Soc. Am. A* **18**(3), 497–505 (2001).
2. A. Dubra, C. Paterson, and C. Dainty, "Study of the tear topography dynamics using a lateral shearing interferometer," *Optics Express* **12**(25), 6278–6288 (2004).
3. L. Koechlin, "Topographie cornéenne par mesure de front d'onde," presented at Journées SF2A "ASHRA", Bordeaux, France 2003.
4. F. Roddier, "Wavefront sensing and the irradiance transport equation," *Applied Optics* **29**, 1402–1403 (1990).
5. K. Ichikawa, A. W. Lohmann, and M. Takeda, "Phase retrieval based on the irradiance transport equation and the Fourier transform method: experiment," *Applied Optics* **27**(16), 3433–3436 (1988).
6. F. Roddier and C. Roddier, "Wavefront reconstruction using iterative Fourier transforms," *Applied Optics* **30**(11), 1325–1327 (1991).

List of Figure Captions

Fig. 1. Schematic diagram of the optical system.

Fig. 2. Corneal topography of an astigmatic eye represented in terms of radial curvature.

Fig. 3. Individual frames from different series showing the tear film topography after removal of first and second order Zernike terms. (a) shows the tear film at the start of a blink (greyscale range: $9\mu\text{m}$), and (b) shows a bubble on the tear film (bottom right, greyscale range: $0.3\mu\text{m}$.)

Fig. 4. RMS error evolution of the wavefront transmitted through the tear film over 10s series. (a) Subject blinked 3 times during series acquisition. (b) Subject refrained from blinking.

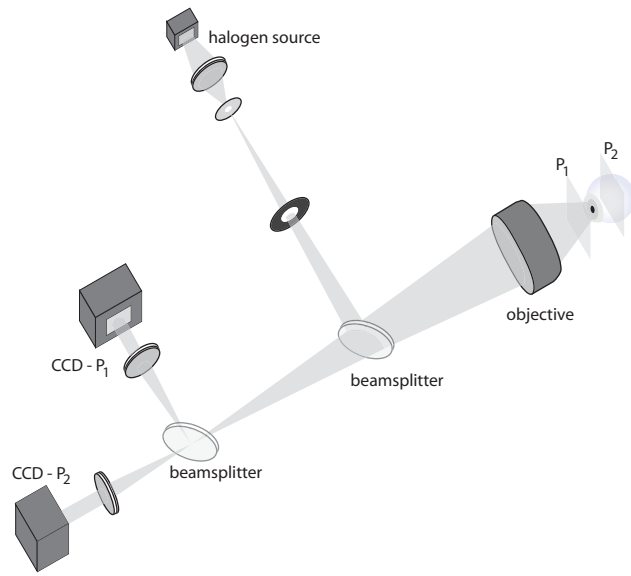


Fig. 1. Schematic diagram of the optical system. GruppettaF01.eps

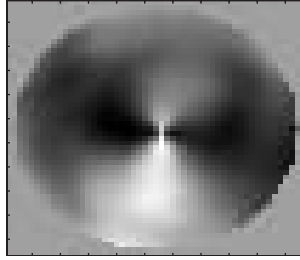


Fig. 2. Corneal topography of an astigmatic eye represented in terms of radial curvature. GruppettaF02.eps

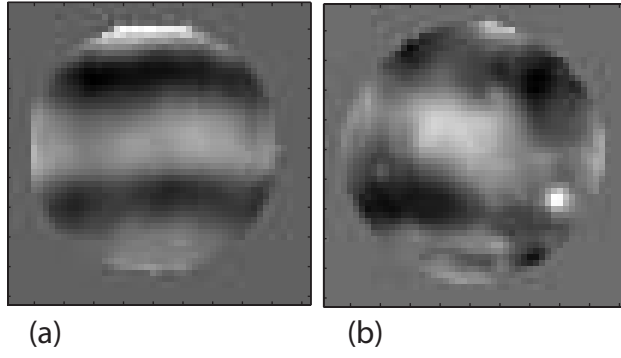


Fig. 3. Individual frames from different series showing the tear film topography after removal of first and second order Zernike terms. (a) shows the tear film at the start of a blink (greyscale range: $9\mu\text{m}$), and (b) shows a bubble on the tear film (bottom right, greyscale range: $0.3\mu\text{m}$.) GruppettaF03.eps

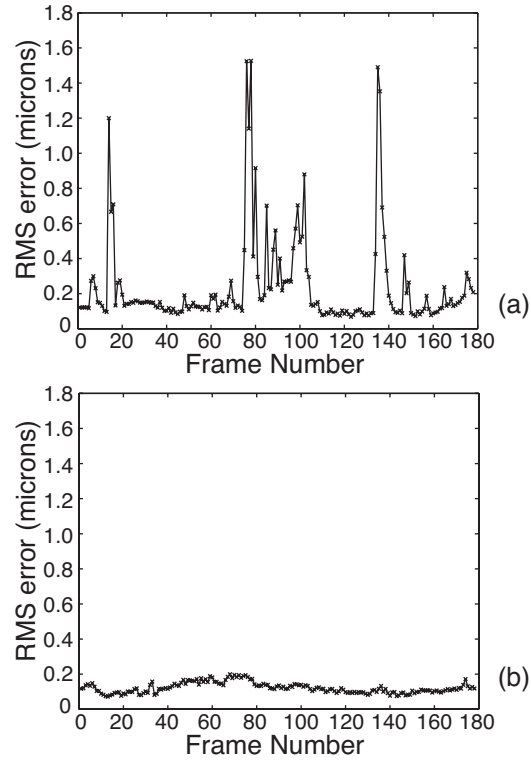


Fig. 4. RMS error evolution of the wavefront transmitted through the tear film over 10s series. (a) Subject blinked 3 times during series acquisition. (b) Subject refrained from blinking. GruppettaF04.eps